Journal of Sound and Vibration (2002) **252**(1), 37–63
doi:10.1006/jsvi.2001.4025, available online at http://www.idealibrary.com on IDEAL®

INERTIAL- AND FLOW-INDUCED ACOUSTIC MODES COUPLING IN UNSTEADY-ROTATING CYLINDRICAL FLUID-FILLED CAVITIES

D. Ecotiere, M. Bruneau and N. Tahani

Laboratoire d'Acoustique de l'Université du Maine, U.M.R.C.N.R.S. 6613, *Université du Maine, Avenue Olivier Messiaen*, 72085 *Le Mans Cedex* 09, *France. E-Mail: david.ecotiere@univ-lemans.fr*

(*Received* 27 *November* 2000, *and in final form* 29 *August* 2001)

A previous investigation has used a procedure for analyzing the transient behaviour of acoustic gyrometers, providing advances in "inertial–acoustic" theory and modelling. The approximate behaviour of the Coriolis acoustic modes coupling in a gyroscopic fluid-filled cylindrical cavity, for a very fast variation of the rotation rate of the cavity, has been derived, showing, after the stabilization of the rotation rate of the fluid, an asymptotic value of the sensitivity in good agreement with the theoretical steady state value and with the experimental result for steady rotation. However, the parameters which govern the transient response, its shape and its characteristic stabilization time, were not fully identified. Especially, the analysis does not predict recent experimental results, which show a stabilization time for the transient response of the gyro much shorter than the stabilization of the unsteady circular flow created when the walls of the cavity are set impulsively (Heaviside step function) in rotation. Thus, it is the aim of the present paper to investigate more deeply, analytically, the transient behaviour of the acoustic gyro, using a revisited description for the inertial–acoustic modes coupling which conveys significant improvements and introducing new features (as the flow-induced acoustic modes coupling) neglected in the previous investigation. The theoretical results are in good agreement with the experimental results now available; they also permit both to interpret the physical phenomena which underlie the "inertial–acoustic" transient process and to address requirements that have to be taken into account in the design of acoustic gyros.

1. INTRODUCTION

Nowadays, there exists an understanding that inertial coupling between acoustic modes inside rotating fluid-filled resonant cavities occurs which provides methodology for designing new sensors (acoustic gyrometers) involving smaller dimensions [1], lower manufacturing costs and lower power consumption, as well as higher reliability and improved lifetime. The physical mechanisms which have been investigated until now are those related to the nature of this coupling, in the frequency domain [2–5] and more recently in the time domain [6].

In fact, it has already been established that the stationary angular velocity of these acoustic gyrometers can be obtained directly from the measurement of the acoustic pressure (the acoustic energy being provided by a localized source set on the wall) using a flush-mounted localized microphone, and requirements that have to be taken into account in the design of acoustic gyros have been addressed from the analysis of the phenomena involved.

0022-460X/02/$35.00

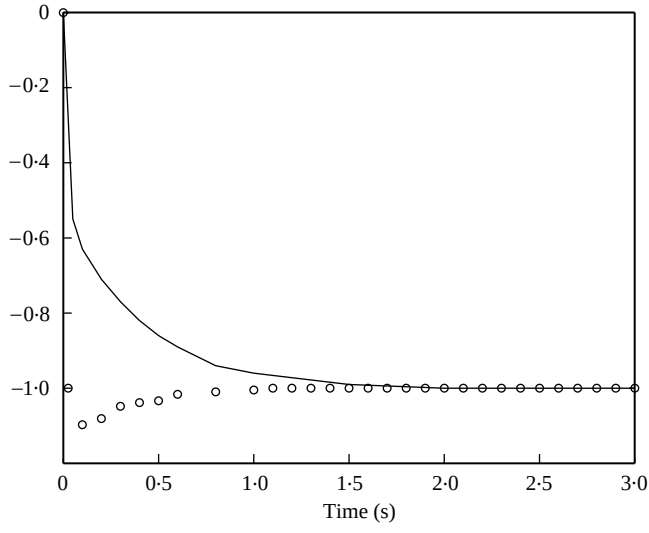

Figure 1. Root mean square of the amplitude of the normalized total acoustic pressure at the location of the measurement microphone ($r = R, \phi = \pi/2$) as functions of the time (transient response of the gyro): ——, theoretical results of the previous theory [6]; ○○○, experimental results.

However, the parameters which govern the transient response, especially the first part of the transient (the early beginning), were not conveniently identified because an important part of the solution of the problem was not obtained, neither analytically nor numerically. (Previous theoretical results [6] are given in Figure 1.) Due to the fact that these parameters govern the shape of the transient response, especially the stabilization time, it is most important to have an analytical model to describe the response of the acoustic gyro for strong variations of the rotation rates.

Therefore, a procedure for analyzing these transient processes is needed, focusing on the stabilization part (typically here 100 ms for the classical 1 cm^3 volume of the cavity used) but valid over the transient response of each factor involved in the physical mechanisms (approximately 3 s). This analysis provided in the present paper departs from the previous one established in 1998 [6] in that (1) a simplified space–time description of the unsteady rotational velocity gradient of the fluid is used to emphasize the physical behaviour of the earliest part of the transient, (2) a revisited description of the inertial–acoustic coupling is proposed which conveys significant accomplishments, (3) a new factor, which takes into account the effect of the non-uniform rotating flow on the acoustic field created by the localized primary acoustic source (providing energy to the system) is introduced, making important practical differences on the final result and allowing one to explain the experimental results available recently. Moreover, because the unsteady, and r-dependent, variations of the rotation rate $\Omega(\mathbf{r}, t)$ of the fluid that occur during the transient response of the acoustic gyrometer and the characteristic time for an acoustic resonance to rise in the cavity are band-limited processes, they are associated with slow variations compared with the acoustic pressure or acoustic velocity variations. Thus, the rotation rate $\Omega(r, z, t)$ and the acoustic transient response are expressed in terms of their samples where the sampling period is the period of the acoustic signal T. This allows an analysis of the acoustic problem, in each interval T, as a stationary one, the acoustical primary source being of time periodic nature, which leads to more tractable calculations than those used in the previous paper mentioned above [6].

Thus, the aim of the present work is to investigate analytically the transient behaviour of the acoustic rate gyro when the cylindrical cavity is suddenly set in rotation around its axis. The rotation rate of the walls of the cavity involving the Heaviside step function, the fluid elements acquire velocities gradually: the unsteady motion of the fluid can be described as a circular flow $\Omega(r, z, t)$ leading slowly to (after several seconds) the ultimate state of rigid-body rotation (when the cylinder and the fluid rotate together with a uniform angular velocity Ω_0), according to a diffusing process from the walls of the cavity to its centre. Because this transient variation of the rotation of the fluid $\mathbf{\Omega}(r, z, t)$ occurs only near the walls at the beginning of the transient, during this period the inertial–acoustic modes coupling takes place essentially near the boundaries, emphasizing the role played, in several inertial factors, by the thermoviscous boundary layers, where the entropic and vortical components of the particle velocity reach the same level as the acoustic component.

The final goal of the paper is to analyze both the behaviour of each so-called inertial factor generating the coupled inertial acoustic resonant standing wave, coupled to the resonant wave generated by the loudspeaker, and the effect of the non-uniform rotating flow on the field created by the loudspeaker, which gives a measure of the rotation rate of the gyrometer.

Note that part of the fundamental theory presented in the next two sections closely follows, but completes and shortens, sections two and three of the previous paper on the transient behaviour of acoustic gyrometers [6]: it provides the basic equations of the whole problem. Nevertheless, as mentioned above, a more complete and somewhat different approach (which is part of the aim of the next two sections) is taken to derive different solutions for both the unsteady circular flow and the "acoustic" motion (the word "acoustic" being understood here globally because it includes the thermal and vortical motions which accompany the acoustic movement itself); these solutions greatly improve the presentation of the subsequent theory and finally provide additional theoretical results, which are in agreement with the experimental results now available.

2. THE ACOUSTIC GYROMETER: DEVICE AND QUALITATIVE PRESENTATION OF THE MECHANISMS INVOLVED

An acoustic rate gyro provides output signals that are measures of angular rates with respect to an inertial frame. The heart of the acoustic gyros under consideration comprises thin cylindrical cavities (see Figure 2) filled with gas under one or several bars. The radius of the cavities have the same order of magnitude as the wavelength of the acoustic perturbation generated in it, and the height of the cavity is much smaller than the radius and much greater than boundary layer thicknesses. The experimental results reported at the end of this paper have been obtained with a cavity 1·4 cm in diameter with a height of 4 mm, filled with a suitable working gas (see for example reference [2]) that is here SF6 under 2·5 bar. Using an acoustic driver coupled to the cavity through a hole roughly 0·05 cm in diameter set at the azimuthal co-ordinate $\phi = 0$, the gas within the cavity is excited to generate an harmonic acoustic standing wave (at the angular frequency ω_1), corresponding to the resonance of the first azimuthal mode labelled "c" and given by the eigenfunction $J_1(\gamma_{10} r/R) \cos\phi$ corresponding to the values (0, 1, 0) of the quantum numbers (n_r, n_ϕ, n_z), respectively, where J_1 is the first order cylindrical Bessel function of the first kind, γ_{10} the first zero of the first derivative of $J_1(\gamma_{10} r/R)$ with respect to the radial co-ordinate r, R the radius of the cavity. Actually, the viscous and thermal dissipation in the boundary layers are taken into account in the formalism presented in the following sections.

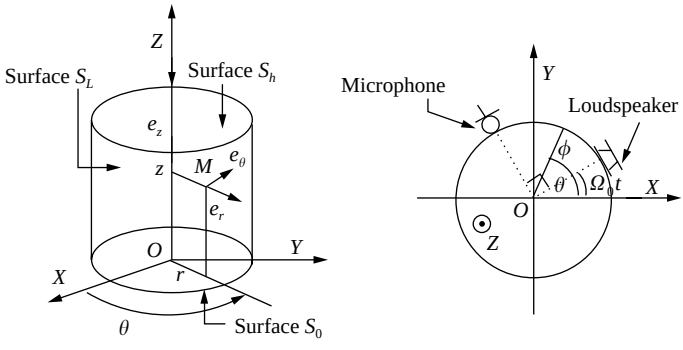

Figure 2. Shape of the cavity; reference frames: inertial $OXYZ$ and non-inertial (M, $\mathbf{e}_r$, $\mathbf{e}_\theta$, $\mathbf{e}_z$); localization of the transducers; notations.

When the cavity rotates around the z-axis of the cylindrical cavity, the angular velocity $\mathbf{\Omega}(r, z, t)$ of the non-inertial frames linked to the particles of fluid, with respect to the inertial frame, depends on both the localization of the particle in the cavity and the time; three main effects must be considered (sections 5 and 6 of the present paper): the dependence of the main field created by the loudspeaker on this non-uniform rotating flow, the Coriolis effect, and the effect of the acceleration associated to the time rate of change of the rotational velocity ($\mathrm{d}\Omega/\mathrm{d}t$) on the acoustic field. (The effect of the centripetal acceleration, proportional to Ω^2 times the particle displacement, does not contribute to the acoustic field detected by the measurement microphone set at $\phi = \pi/2$.) The phenomena involved lead to energy transfer from the mode labelled "c" mentioned above to the orthogonal mode labelled "s" given by the eigenfunction $\mathrm{J}_1(\gamma_{10}\, r/R)\sin\phi$ which can be measured with a microphone set at the point $\phi = \pi/2$, even if its amplitude is much lower than the amplitude of the primary mode "c" generated by the loudspeaker (which is null at $\phi = \pi/2$). (These two modes "c" and "s" are almost sufficient to describe a solution for the acoustic response of the rotating cavity, in the "ideal" case of a perfectly shaped cavity; actually, in order to take into account unavoidable small perturbations, more terms can be included into the eigenfunctions expansion which is used to describe the acoustic field [3].)

Moreover, the inertial forces $\mathbf{f}$ can be interpreted in the acoustic wave equation as a source term given by (see section (6))

$$\frac{1}{\rho_0}\nabla\cdot\mathbf{f} = \nabla\cdot\left[2\mathbf{\Omega}\times\mathbf{v} + \mathrm{d}_t\mathbf{\Omega}\times\frac{\mathbf{v}}{\mathrm{i}\omega_1}\right]$$
$$= -\left(2\Omega + \frac{1}{\mathrm{i}\omega_1}\mathrm{d}_t\Omega\right)(\nabla\times\mathbf{v})_z - \left(2\partial_r\Omega + \frac{1}{\mathrm{i}\omega_1}\partial_r\partial_t\Omega\right)v_\phi, \qquad (1)$$

emphasizing that the vortical component $\mathbf{v}_v$ of the particle velocity $\mathbf{v}(\nabla\times\mathbf{v} = \nabla\times\mathbf{v}_v)$ plays an important role in the inertial coupling. This vortical component is almost negligible everywhere except inside the viscous boundary layers, which therefore play an important role in the process. Hence, the contribution of the energy transfer from the mode "c" to the mode "s" due to the inertial phenomena takes place inside the whole cavity, and especially in the very thin boundary layers. On the other hand, the strength of this "inertial resonant field" created in the cavity is proportional to both the amplitude of the primary resonant mode "c" generated by the loudspeaker and the rotation rate of the cavity [2, 3]. Then, one can say that the transfer function between the output signal of the microphone set at $\phi = \pi/2$, which measures the amplitude of the mode "s", and the output signal of another

microphone set at $\phi = \pi$ which measures the amplitude of the primary mode "c", provides the value of the rotation rate Ω, but only after the short period which corresponds to the characteristic time for an acoustic resonance to rise in the cavity (section (6)).

The theory developed in the following sections, devoted to the description of both the inertial–acoustic coupling and the effect of the non-uniform rotating flow, when strong unsteady variations of the rotation rates (which depend both on the time and the location in the cavity) occur, provides details needed to understand more deeply the precedent summary.

3. THE FUNDAMENTAL PROBLEM

3.1. THE BASIC PROBLEM

The cavity studied is a cylindrical one (height h, radius R), in which transducers are flush mounted to the base ($z = 0$) near the circular lateral wall ($r \simeq R$). The origin of the inertial reference frame used is located at the centre of the base of the cylinder. The corresponding natural co-ordinates chosen are Cartesian (X, Y, Z) or cylindrical (r, θ, z) and the (**Oz**/**OZ**) axis is aligned along the geometric axis of the cylinder, which itself is coincident with the rotation vector of the moving gas within the cavity $\mathbf{\Omega}(r, z, t)$ (see Figure 2).

The gas of the cavity is excited by the loudspeaker, set at the azimuthal angle $\theta = \Omega_0 t$ where Ω_0 is the rotation rate of the wall, non-null at times $t \geqslant 0$ (note that $\phi = \theta - \Omega_0 t$ if $t \geqslant 0$, and $\phi = \theta$ if $t \leqslant 0$). It is excited on its first acoustic azimuthal mode (0, 1, 0) labelled "c", in such a way that the measurement microphone, which is located at a right angle ($\phi = \pi/2$) from the loudspeaker, sets on a node of pressure of that mode when the cavity is at rest ($t < 0$).

At time $t = 0$, the cavity is set impulsively in rotation, with its angular speed being brought from zero to Ω_0. Then, the fluid goes through a transient stage where particles are gradually driven by the walls, acquiring the angular velocity $\Omega(r, z, t)$, until reaching the ultimate state of rigid-body rotation (when the cylinder and the fluid rotate together with the uniform angular velocity Ω_0). As the system has an axial symmetry, this angular velocity is assumed to be independent of the azimuthal co-ordinate.

3.2. EQUATIONS OF MOTION

The motion of the fluid can be described as the superposition of a circular flow linked to the boundary condition expressing the rotation of the walls of the cavity, and an acoustic perturbation generated by the acoustic source which is the rate of mass density creation "$\rho_T q$" (this acoustic field being largely perturbed by the rotation of the gyro and the subsequent non-homogeneous circular flow). It is governed by the following set of fundamental equations:

the Stokes–Navier equation,

$$\rho_T \mathrm{d}_t \mathbf{V}_T = -\nabla P_T + \mu \Delta \mathbf{V}_T + \left(\eta + \frac{\mu}{3}\right) \nabla(\nabla \cdot \mathbf{V}_T), \tag{2}$$

the mass conservation equation,

$$\mathrm{d}_t \rho_T + \rho_T \nabla \cdot \mathbf{V}_T = \rho_T q, \tag{3}$$

the heat conduction equation,

$$\rho_T T \mathrm{d}_t S_T = \lambda \Delta T \tag{4}$$

and the usual thermodynamical state equations, where

$$\mathrm{d}_t \equiv \partial_t + \mathbf{V}_T \cdot \nabla \tag{5}$$

is the material derivative.

Here, $\mathbf{V}_T$, ρ_T, P_T, S_T and T are, respectively, the particle velocity, the density, the pressure, the entropy per unit volume and the temperature associated to the fluid motion, λ, μ and η are, respectively, the coefficients of thermal conductivity, shear viscosity and bulk viscosity of the fluid.

3.3. THE UNSTEADY CIRCULAR FLOW

The unsteady circular flow is governed by the set of equations (2) and (3) in the absence of any acoustic source. Upon neglecting the fluid compressibility ($\nabla \cdot \mathbf{V} = 0$) and assuming consequently that the radial component V_r of the particle velocity (denoted $\mathbf{V}$) vanishes (pure shear circular flow), the only non-vanishing component of the velocity $\mathbf{V}$ is [6]

$$V_\theta(r, z, t) = \Omega(r, z, t) r, \tag{6}$$

where Ω is the angular velocity of the particles set at the distance r from the centre and the co-ordinate z from the wall $z = 0$, and the radial and azimuthal components of the Stokes–Navier equation (2) can be written, respectively, as [6]

$$\frac{V_\theta^2}{r} = \frac{1}{\rho_0}\frac{\partial P}{\partial r}, \quad \frac{\partial V_\theta}{\partial t} = \nu\left(\frac{\partial^2}{\partial r^2} + \frac{1}{r}\frac{\partial}{\partial r} - \frac{1}{r^2} + \frac{\partial^2}{\partial z^2}\right) V_\theta, \tag{7}$$

where $\nu = \mu/\rho$ is the kinematic viscosity coefficient.

The solution V_θ of the second equation (7) which satisfies the boundary conditions (U(t) being the Heaviside step function)

$$V_\theta(r, z = 0, t) = V_\theta(r, z = h, t) = \Omega_0 r \mathrm{U}(t), \tag{8a}$$

$$V_\theta(r = R, z, t) = \Omega_0 R \mathrm{U}(t), \tag{8b}$$

can be expressed as a double Fourier–Bessel expansion [7]:

$$\frac{V_\theta}{r}(r, z, t) = \Omega = \Omega_0 \left[1 + \frac{R}{r} \sum_{m=1,3,\ldots,} \sum_{n=1,2,\ldots,} \frac{8}{m\pi} \sin\left(\frac{m\pi}{h} z\right) \frac{\mathrm{J}_1(\lambda_n/R) r}{\lambda_n \mathrm{J}_0(\lambda_n)} \mathrm{e}^{-k_{mn}^2 \nu t}\right] \mathrm{U}(t) \tag{9}$$

with $k_{mn}^2 = (m\pi/h)^2 + (\lambda_n/R)^2$, and where the coefficients λ_n are the zeros of the first order cylindrical Bessel function of the first kind ($\mathrm{J}_1(\lambda_n) = 0$). The first relationship (7) gives the radial pressure gradient created by the centripetal acceleration; its effect is neglected in the range of rotation rate under consideration in current application.

The field of the normalized angular velocity $\Omega/\Omega_0 = (V_\theta/r)/\Omega_0$ of the unsteady circular flow, calculated with 30×30 modes $m \times n$ in expansion (9), is given in Figure 3, showing its shape as a function of the normalized co-ordinates $z_h = z/h$ and $u_r = r/R$ for four values of the time t (0·01, 0·1, 0·3, 1 s). It is clear that the unsteady rotational velocity gradient becomes roughly negligible only after a few seconds. But fortunately, as will be shown at the end of the present paper, the transient response of the gyro is much shorter than that (between 10 and 100 ms for the cavity used in the experimental investigation).

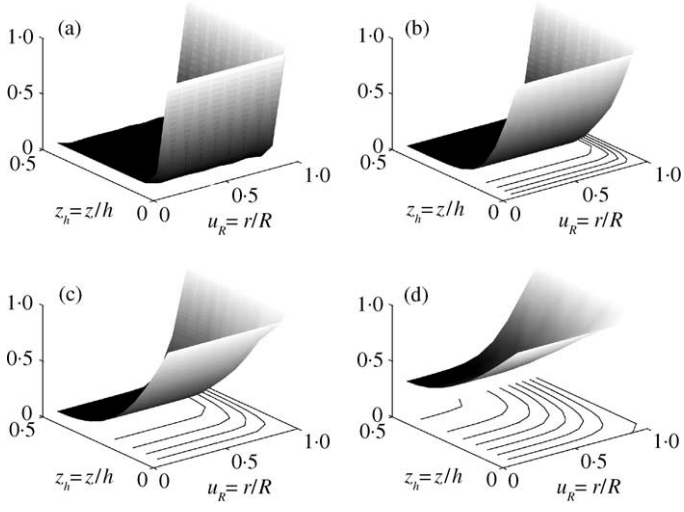

Figure 3. Field of the normalized angular velocity Ω/Ω_0 of the unsteady circular flow, calculated with 30×30 modes ($m \times n$) in expansion (9), as a function of the normalized co-ordinates $z_h = z/h$ and $u_R = r/R$ for four values of the time t: (a) $t = 0{\cdot}01$ s; (b) $t = 0{\cdot}1$ s; (c) $t = 0{\cdot}3$ s; (d) $t = 1$ s.

Then, it is most important both to obtain accurate computational results for this transient which adequately agree with the experimental data over a large time range (here typically from 0 to 3 s) using expression (9) for the rotation rate Ω, and to carry out analytical studies in order to interpret in detail each phenomenon involved in the final results; even the analytical results which follow would be approximately valid over a short time interval provided that it covers the transient response of the gyro (here up to 100 ms). Such extremely useful analytical studies presented, in the next sections, are derived from a simplified and approximate expression for the rotation rate Ω which is valid greatly over the transient response of the gyro (until 300 ms for the gyro used in the experiments reported here). During this period, i.e., the early beginning of the transient regime for the rotating cavity, the angular velocity Ω is null everywhere except near the walls because the fluid elements acquire velocity V_θ gradually according to a diffusion process (equation (7)) from the walls of the cavity to its centre. Hence, this diffusion process can be assumed to take place from each wall ($z = 0, h$ and $r = R$) independently, that is without any interaction between them. This approximation enables one to simplify greatly the expression for the rotation rate Ω close to each wall, valid for a time interval which, as mentioned previously, widely covers the transient response of the gyro, namely [7, 8] (Appendix A):

$$\frac{\Omega^{(0/h)}}{\Omega_0} = \operatorname{erfc}\left(\frac{x}{2\sqrt{\nu t}}\right) \mathrm{U}(t), \tag{10}$$

$$\frac{\Omega^{(R)}}{\Omega_0} = \left(\frac{R}{r}\right)^{3/2} \operatorname{erfc}\left(\frac{R-r}{2\sqrt{\nu t}}\right) U(t). \tag{11}$$

Here, the rotation rates near the surfaces $z = 0$ ($x = z$) and h ($x = h - z$) are, respectively, denoted by subscripts (0) and (h), and the rotation rate near the surface $r = R$ is denoted by the subscript (R). The function $\operatorname{erfc}(y) = 1 - (2/\sqrt{\pi}) \int_0^y \mathrm{e}^{-u^2}\, \mathrm{d}u$ is the complementary error function.

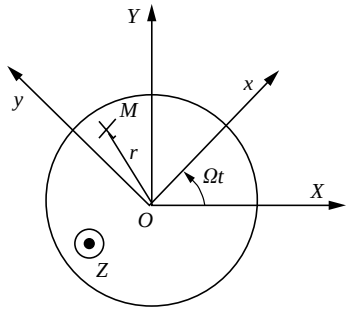

Figure 4. Reference frame: fixed frame (O, X, Y, Z) and moving frame (O, x, y, z).

3.4. FUNDAMENTAL EQUATIONS GOVERNING THE ACOUSTIC MOTION

In the acoustic gyro, the whole motion of the fluid (represented by the particle velocity $\mathbf{V}_T$) includes the unsteady circular flow ($\mathbf{V}$) presented in the previous section 3.3 and an "acoustic" motion ($\mathbf{v}$), the word "acoustic" being taken here globally because it includes the thermal ($\mathbf{v}_h$) and vortical ($\mathbf{v}_v$) motions which accompany the acoustic movement itself ($\mathbf{v}_a$). The instantaneous position of a particle is described by means of the vector $\mathbf{OP} = \mathbf{OM} + \mathbf{MP}$, where $\mathbf{OM}$ is the position vector of the particle driven along the circular streamlines of the flow without acoustic displacement and where $\mathbf{MP}$ represents the displacement $\boldsymbol{\xi}$ of the element of fluid due to the acoustic motion. As the fundamental equations (2)–(5) which describe the particle motion are expressed in an inertial reference frame, the operator "d_t" giving the material derivative will now be denoted "$(d_t)_i$", and the particle velocity and the acceleration associated to the global motion are written, respectively, as

$$\mathbf{V}_T = (\mathrm{d}_t)_i \mathbf{OP}, \quad (\mathrm{d}_t)_i \, \mathbf{V}_T = (\mathrm{d}_{tt}^2)_i \mathbf{OP}. \tag{12, 13}$$

In order to reveal (among others) the expected inertial factors explicitly, the equations of motion are expressed by using a moving reference frame (m), chosen in such a way that it is linked at each time t to the unsteady rotational motion $\Omega(r, z, t)$ of the fluid elements located at the same distance r and the same z-co-ordinate on the z-axis (i.e., situated on the same circular streamline), the origin of this moving frame being the same as the one of the fixed reference frame (Figure 4). Then, the velocity and the acceleration of the particle relative to the inertial frame can be expressed as functions of quantities relative to the moving frame as

$$\mathbf{V}_T = (\mathrm{d}_t)_i \mathbf{OP} = [(\mathrm{d}_t)_m + \boldsymbol{\Omega} \times] \, \mathbf{OP} = \mathbf{v} + \boldsymbol{\Omega} \times \mathbf{OP}, \tag{14}$$

$$\begin{aligned} (\mathrm{d}_t)_i \, \mathbf{V}_T &= [(\mathrm{d}_t)_m + \boldsymbol{\Omega} \times] \, \mathbf{V}_T \\ &= (\mathrm{d}_t)_m \, \mathbf{v} + 2\boldsymbol{\Omega} \times \mathbf{v} + \mathrm{d}_t \boldsymbol{\Omega} \times \mathbf{OP} + \boldsymbol{\Omega} \times (\boldsymbol{\Omega} \times \mathbf{OP}), \end{aligned} \tag{15}$$

where $\boldsymbol{\xi}$ and $\mathbf{v} = (\mathrm{d}_t)_m \boldsymbol{\xi}$ represent, respectively, the displacement and the velocity of the particle due to the "acoustic" motion, $(\mathrm{d}_t)_m$ being the operator giving the material derivative in the moving frame. (The time derivative of the rotation rate Ω satisfying the property $(\mathrm{d}_t)_i \boldsymbol{\Omega} = (\mathrm{d}_t)_m \boldsymbol{\Omega}$, it can be written as either $\mathrm{d}_t \boldsymbol{\Omega}$ or $\partial_t \boldsymbol{\Omega}$.)

Therefore, invoking the properties of the position vector $\mathbf{OM}$ and the associated velocity $\mathbf{V} = \mathbf{V}_T - \mathbf{v}$ of the particle driven along the circular streamlines of the flow without acoustic

displacement, namely

$$\nabla \cdot \mathbf{V} = \nabla \cdot (\dot{\mathbf{\Omega}} \times \mathbf{OM}) = 0, \tag{16}$$

$$\begin{aligned}(\mathrm{d}_t)_i \mathbf{V} &= \mathrm{d}_t \mathbf{\Omega} \times \mathbf{OM} + \mathbf{\Omega} \times (\mathrm{d}_t)_i \mathbf{OM} \\ &= \mathrm{d}_t \mathbf{\Omega} \times \mathbf{OM} + \mathbf{\Omega} \times (\mathbf{\Omega} \times \mathbf{OM})\end{aligned} \tag{17}$$

and (the Navier–Stokes equation where P is the pressure created by the centripetal acceleration, equation (7))

$$(\mathrm{d}_t)_i \mathbf{V} = -\frac{1}{\rho_0} \nabla P + \nu \Delta (\mathbf{\Omega} \times \mathbf{OM}) \tag{18}$$

and then using equations (14) and (15), and assuming that the acoustic density $\rho = \rho_T - \rho_0$ is much lower than the unperturbed acoustic density and that $\mathbf{\Omega} \times \mathbf{OP}$ is much lower than the "acoustic" particle velocity $\mathbf{v}$ for the range of the rotation rate considered in current application, the Navier–Stokes equation (2) yields the relevant corresponding equation for the acoustic pressure $p = P_T - P$, the "acoustic" particle velocity $\mathbf{v}$ and the "acoustic" particle displacement $\boldsymbol{\xi}$ [6]:

$$\rho_0 [(\mathrm{d}_t)_m \mathbf{v} + 2\mathbf{\Omega} \times \mathbf{v} + \mathrm{d}_t \mathbf{\Omega} \times \boldsymbol{\xi} + \mathbf{\Omega} \times (\mathbf{\Omega} \times \boldsymbol{\xi})] = -\nabla p + \mu \Delta \mathbf{v} + (\eta + \mu/3) \nabla \nabla \cdot \mathbf{v}. \tag{19}$$

When considering the stationary regime, the cylinder and the fluid rotating together with a uniform angular velocity $\mathbf{\Omega}_0$, the fluid and the transducers (the localized acoustic source and the microphone) rotate at the same angular velocity $\mathbf{\Omega}_0$ and each one remain continuously motionless with regard to the others; then within the framework of the linear acoustics, the material derivative with respect to the time in the moving frame (m) denoted $(\mathrm{d}_t)_m$ is equal to the partial derivative $(\partial_t)_m$ in the same frame. But, during the transient regime, when the rotational velocity $\Omega(r, z, t)$ of the fluid is non-uniform and differs everywhere (except for $r = R$, $z = 0$ and h) from the angular velocity Ω_0 of the walls and so from the angular velocity Ω_0 of the transducers, each particle has its own relative movement with respect to the transducers, given by the angular velocity $[\Omega(r, z, t) - \Omega_0]$; therefore, the local velocity of the frame linked to the fluid with respect to the velocity of the frame linked to the transducers is given by $[\Omega(r, z, t) - \Omega_0]r$, and the requisite expression for the material derivative $(\mathrm{d}_t)_m$ is

$$(\mathrm{d}_t)_m \simeq \partial_t + (\Omega - \Omega_0) r \mathbf{e}_{\phi} . \nabla = \partial_t - \delta\Omega \ \partial_{\phi}, \tag{20}$$

where $(\partial_t)_m$ is denoted ∂_t for simplicity, $\delta\Omega = \Omega_0 - \Omega(r, z, t)$, ∂_{ϕ} being the partial derivative with respect to the azimuthal co-ordinate $\phi = \theta - \Omega_0 t$ (see Figure 2).

The correction term $\delta\Omega \ \partial_{\phi}$, which takes into account the effect of the non-uniform rotating flow on the acoustic field directly created by the localized primary acoustic source (providing energy to the system), was assumed to be negligible in the previous paper [6]; in fact, as demonstrated below, it plays an important role during the transient period of the gyro, at the beginning of the transient of the rotating flow.

Finally, the "acoustic" movement (that is the sum of the acoustic, entropic and vortical movement) is governed by a set of three equations including the conservation of mass equation (3) and the heat conduction equation (4), both restricted to the "acoustic" field and expressed in the moving frame, and also the Stokes–Navier equation (19) in accordance

with equation (20), namely

$$\left[\frac{1}{c_0}(\partial_t - \delta\Omega\partial_\phi) - l'_v\Delta\right]\mathbf{v} + \frac{1}{\rho_0 c_0}\nabla p = -\frac{\mathbf{\Gamma}}{c_0} + \left(\frac{\eta}{\rho_0 c_0} + \frac{1}{3}l'_v\right)\nabla\nabla\cdot\mathbf{v}, \tag{21}$$

$$(\partial_t - \delta\,\Omega\partial_\phi)\rho + \rho_0\nabla\cdot\mathbf{v} = \rho_0 q, \tag{22}$$

$$\left[\frac{1}{c_0}(\partial_t - \delta\Omega\partial_\phi) - l_h\Delta\right]\tau = \left(\frac{\gamma - 1}{\hat{\beta}\gamma c_0}\right)\partial_t p \tag{23}$$

with

$$\rho = (p - \hat{\beta}\tau)\,\gamma/c_0^2 \quad \text{(state equation)}, \tag{24}$$

$$\mathbf{\Gamma} = \mathbf{\Gamma}_c + \mathbf{\Gamma}_a + \mathbf{\Gamma}_e, \tag{25}$$

$$\mathbf{\Gamma}_c = 2\mathbf{\Omega}\times\mathbf{v}, \quad \mathbf{\Gamma}_a = \partial_t\mathbf{\Omega}\times\partial_t^{-1}\mathbf{v}, \quad \mathbf{\Gamma}_e = \mathbf{\Omega}\times(\mathbf{\Omega}\times\partial_t^{-1}\mathbf{v}), \tag{26}$$

$$l'_v = \frac{v}{c_0} = \frac{\mu}{\rho_0 c_0}, \quad l_h = \frac{\lambda}{\rho_0 C_p c_0}, \tag{27}$$

where in the inertial correction terms $\mathbf{\Gamma}_a$ and $\mathrm{A}\mathbf{\Gamma}_e$, the "acoustic" displacement $\boldsymbol{\xi} = (\mathrm{d}_t^{-1})_m\mathbf{v}$ is written as $\boldsymbol{\xi} \simeq \partial_t^{-1}\mathbf{v}$, disregarding the correction term linked to the motion of the fluid (in equation (20)), and where C_p is the heat coefficient at constant pressure per unit of mass, c_0 the adiabatic speed of sound, γ the specific heat ratio and $\hat{\beta}$ the increase in pressure per unit increase in temperature at constant density.

The regular solutions of equations (21)–(23), when the time-periodic source activity is given by the harmonic rate of creation of fluid per unit volume of the localized loudspeaker set on the cylindrical wall

$$q = Q\cos\omega_1 t = Q_0\frac{\delta(r - R)}{r}\delta(\phi)\cos\omega_1 t, \tag{28}$$

invoking expression (9) or (10–11) for the rotation rate Ω and subject to the boundary conditions (on the walls $z = 0, h$ or $r = R$) for the temperature variation and the "acoustic" particle velocity, namely

$$\tau = 0 \quad \text{and} \quad \mathbf{v} = \mathbf{0} \tag{29}$$

are the appropriate results that are needed to interpret the experimental data available (the acoustic pressure given by the measurement microphone set at $\phi = \pi/2$); the remainder of the paper is devoted to that purpose.

4. INTRODUCTION TO THE ACOUSTIC WAVE MOTION AND THE SUITABLE GREEN FUNCTION

4.1. INTRODUCTION

Inspection of equation (21) with consideration of the orders of magnitude of the quantities involved, reveals that the perturbations which depend on both the fluctuating inertial phenomena ($\mathbf{\Gamma}$) and the effects of the non-uniform rotating flow on the acoustic field directly created by the loudspeaker ($\delta\Omega, \partial_\phi\mathbf{v}$) can be expected to be much lower than the main acoustic field, in the range of rotation rate Ω under consideration in current application and for the angular frequency ω_1 of the monochromatic wave tuned on the first

azimuthal mode of the cavity ($\Omega \ll \omega_1 \simeq 10^5\ \mathrm{s}^{-1}$ for the kind of gyro used in the experiment reported here). Hence the effects (acoustic modes coupling) of these factors, which depend on the unknown acoustic velocity itself, can be calculated by using the Born approximation, that is by assuming that the expression of the acoustic velocity in these terms can be replaced by its expression for $\Omega = 0$. Therefore, in the following sections, we proceed with the derivation of the relevant solution of the equations which govern the acoustic field inside the cavity at rest (section 5) before giving (in section 6) approximate solutions for the correction terms which depend on the rotation rate Ω (the most important ones for the purpose of the gyro). Moreover, to reduce the complexity of the remaining problems for the fluid at rest and to obtain explicit representations of the acoustic fields, taking into account the effects of viscosity and thermal conduction, implies that several operations and approximations are carried out in the derivation of the appropriate basic equations involved as well as in their solutions.

The analysis of the cavity excitation relies on modal functions of the domain, together with their related eigenvalues; and a prominent role is given to a Green function, which incorporates these characteristic quantities, to obtain the solutions for both the acoustic field without rotation and the correction terms involved when the cavity rotates. So before solving the problem in the time domain governed by equations (21)–(29) (including equation (9) or (10–11) for Ω) as indicated above, we derive the Green function in the time domain for the non-rotating fluid, expressed as an eigenfunction expansion restricted to the resonant modes of the cavity at the tuned frequency.

4.2. THE GREEN FUNCTION IN THE TIME DOMAIN AND ITS EIGENFUNCTION EXPANSION

In order to increase the acoustic particle velocity of both the main acoustic field (created by the harmonic source) and the associated field (coupled with the main one by the rotation of the cavity) giving the sensitivity of the gyro, the frequency is monitored to make these fields resonant (a microphone set at the angle $\phi = \pi$ from the loudspeaker supplies a feedback signal which maintains these resonances): namely, the angular frequency ω_1 of the monochromatic source is tuned to the first azimuthal mode of the cavity (0, 1, 0). So the Green function has the particularity of presenting its maximum, proportional to the quality factor of the cavity, which must behave accurately in order to provide theoretical amplitudes, for the acoustic pressure, in agreement with the experimental results. It is therefore consequent to express adequately the dissipation processes, namely the viscous and thermal effects in the boundary layers near the rigid walls as well as *a priori* in the bulk of the cavity. The propagation equation for the subsequent Green function is obtained from the set of equations (21)–(23) for $\mathbf{\Gamma} = \mathbf{0}$ and $\delta\Omega = 0$, leading to [9]

$$\left[\left(1 + l_{vh}\frac{1}{c_0}\partial_t\right)\Delta - \frac{1}{c_0^2}\partial_{tt}^2\right] G(\mathbf{r}, \mathbf{r_0}, t, t_0) = -\,\delta(t - t_0)\,\delta(\mathbf{r} - \mathbf{r_0}),\ r \in [0, R],\ z \in [0, h], \quad (30)$$

where the factor $l_{vh} = l_v + (\gamma - 1)l_h$, with $l_v = 1/(\rho_0 c_0)(\eta + 4/3\,\mu)$, accounts for the dissipation process in the bulk of the fluid; and, in order to model the sound absorption in the viscothermal boundary layers, this Green function is chosen to satisfy an appropriate admittance-like boundary condition expressed in the frequency domain for the angular frequency of interest, namely,

$$(\partial_n + \mathrm{i}k_0\beta)\tilde{G}(\mathbf{r}, \mathbf{r_0}) = 0, \quad z = 0 \quad \text{or } h \text{ or } r = R, \quad (31)$$

where $\tilde{G}$ is the Fourier transform of G, $k_0 = \omega/c_0$, ∂_n being the outwardly derivative normal to the wall considered.

It is noteworthy first that such a boundary condition is restricted to fields in cavities whose height and radius are large enough with respect to the boundary layer thicknesses so that these thicknesses are negligible as regards the spatial distribution of the acoustic perturbation obtained (which is valid only outside the boundary layers), and second that the small admittance β depends on the direction characterized by $k_w^{(N)2}$ of the acoustic velocities on the walls, namely

$$\beta = \frac{1+\mathrm{i}}{\sqrt{2}}\sqrt{k}\ [k_w^{(N)2}\sqrt{l_v'} + (\gamma-1)\sqrt{l_h}], \tag{32}$$

so its expression must be used carefully as shown in section 5.1. equation (62).

The analytic Green function in the frequency domain is approximately expressed as an eigenfunction expansion where the orthonormal eigenfunctions $\psi_m(r,\phi,z)$ are solutions of the Neumann boundary value problem

$$(\Delta + \mathrm{k}_m^{02})\,\psi_m(\mathbf{r}) = 0 \quad \text{inside the cavity,}$$
$$\partial_n\psi_m(\mathbf{r}) = 0 \text{ on the boundaries,} \tag{33}$$

leading to [9]

$$\tilde{G}(\mathbf{r},\mathbf{r_0}) = \sum_m \frac{\psi_m(\mathbf{r_0})\psi_m(\mathbf{r})}{k_m^{02} - k^2 + \mathrm{i}k_0\iint_S \beta\psi_m^2\,\mathrm{d}S} \tag{34}$$

with $k = k_0\,(1 - (\mathrm{i}/2)\,\mathrm{k}_0\,l_{vh})$. As the admittance β is very small, the eigenfunctions ψ_m can be considered as a zero order expansion with respect to β; but, nevertheless, the eigenvalues are modified in the denominator of equation (34) with a small term proportional to the mean weighted admittance. Note that as the derivative normal to the walls "∂_n" of the truncated Green function is equal to zero, it might happen that, in some calculations, this approximation would not be relevant, especially when some factors in the integral of coupling (see further) become very important just near the walls. In these cases, the normal derivative "∂_n" must be replaced by its expression ($-\mathrm{i}k_0\beta$) from the boundary conditions (31), when the operator acts on pressure-like analytical functions or by $k\Im(\beta)$ when it acts on the associated real function (the content of this remark is in fact included in the theoretical formulation in the following sections because it follows from the solutions of the acoustic problem for $\Omega = 0$ given in section 5.1, equation (61)).

The Green function in the time domain is given by integrating its expression (34) in the frequency domain, by using the residue integration method, leading to the well-known real causal function

$$G(\mathbf{r},\mathbf{r_0},t,t_0) = c_0^2\,\mathrm{U}(t-t_0)\sum_m \sin(\omega_m(t-t_0))\frac{\mathrm{e}^{-\gamma_m(t-t_0)}}{\omega_m}\,\psi_m(\mathbf{r_0})\,\psi_m(\mathbf{r}), \tag{35}$$

where

$$\omega_m \simeq \omega_m^0 - \gamma_m,\ \omega_m^0 = k_m^0 c_0, \tag{36}$$

and

$$\gamma_m = \frac{c_0}{2\sqrt{2}}\iint_S \frac{\sqrt{2}}{1+\mathrm{i}}\beta\psi_m^2\,\mathrm{d}S + \frac{c_0}{2}\,k_0^2 l_{vh} \simeq \frac{c_0}{2\sqrt{2}}\iint_S \frac{\sqrt{2}}{1+\mathrm{i}}\beta\psi_m^2\,\mathrm{d}S. \tag{37}$$

In this last approximate expression for γ_m, the contribution of the dissipation in the bulk of the fluid $(c_0/2)k_0^2 l_{vh}$ is neglected because it is much lower than the contribution of the

boundaries given by the term involving the integration, which lies over the surface S of the walls, of the weighted specific admittance (using expression (32) for β, $\gamma_m \simeq 50\ \mathrm{s}^{-1}$ which is much greater than $(c_0/2)k_0^2 l_{vh} \simeq 10^{-3}\ \mathrm{s}^{-1}$ for the device studied here). Hence, the factor $l_{vh}\ (1/c_0)\ \partial_t$ can be definitely cancelled in equation (30): the bulk dissipation due to viscous and thermal effects can be neglected in this kind of cavity.

In the following, the Green function expansion is truncated to include only the first two resonant azimuthal modes (as indicated before), namely, upon using the cylindrical co-ordinates,

$$\psi_1^c(r, \phi, z) = N_0^{-1}\, \mathrm{J}_1(k_{10} r) \cos\phi, \tag{38}$$

$$\psi_1^s(r, \phi, z) = N_0^{-1}\, \mathrm{J}_1(k_{10} r) \sin\phi, \tag{39}$$

with

$$N_0 = \mathrm{J}_1(\gamma_{10}) \sqrt{1 - \frac{1}{\gamma_{10}^2}} \sqrt{\pi R^2 \frac{h}{2}}, \tag{40}$$

$$k_{10} = \frac{\gamma_{10}}{R}, \quad \gamma_{10} = 1{\cdot}84, \tag{41}$$

leading to, in the frequency domain, for the angular frequency ω_1 of interest,

$$\tilde{G}(\mathbf{r}, \mathbf{r_0}) = \frac{\psi_1^c(\mathbf{r})\psi_1^c(\mathbf{r_0}) + \psi_1^s(\mathbf{r})\psi_1^s(\mathbf{r_0})}{k_{10}^2 - k_1^2 + (\mathrm{i} - 1)\chi_1^2}, \tag{42}$$

and in the time domain,

$$G(\mathbf{r}, \mathbf{r_0}, t, t_0) = \frac{c_0^2}{\omega_1} \sin(\omega_1 (t - t_0))\, \mathrm{e}^{-\gamma_1 (t - t_0)} \times (\Psi_1^c(\mathbf{r_0})\Psi_1^c(\mathbf{r}) + \Psi_1^s(\mathbf{r_0})\Psi_1^s(\mathbf{r}))\, \mathrm{U}(t - t_0), \tag{43}$$

where

$$\chi_1^2 = k_1 \iint_S \frac{\beta}{1 + \mathrm{i}} \psi_1^2\, \mathrm{d}S = 2k_1 \frac{\gamma_1}{c_0}, \tag{44}$$

$$\gamma_1 = c_0 \sqrt{\frac{k_1}{2}} \left[\frac{1}{h} \left(\sqrt{l_v'} + (\gamma - 1)\sqrt{l_h} \right) + \frac{\gamma_{10}^2}{R(\gamma_{10}^2 - 1)} \left(\frac{1}{\gamma_{10}^2} \sqrt{l_v'} + (\gamma - 1)\sqrt{l_h} \right) \right], \tag{45}$$

the working angular frequency of the gyro $\omega_1 = c_0 k_1$ being equal to $\omega_{10} - \gamma_1 = c_0 k_{10} - \gamma_1$ which is nearly equal to the eigenvalue ω_{10} because the attenuation factor γ_1 is much lower than the resonance angular frequency:

$$c_0 k_1 = \omega_1 \simeq \omega_{10} = c_0 k_{10}. \tag{46}$$

In the remainder of the paper, the eigenvalue ω_{10}, used for simplicity of the calculation because it is given by its simple expression $(c_0\, \gamma_{10}/R)$, means the approximate value of the true angular frequency ω_1 (the angular resonant frequency). The direction $k_w^{(N)2}$ of the acoustic velocities on the walls (equation (32)) has been replaced, in expression (45) of the attenuation factor, by its expressions, namely $(1/\gamma_{10}^2)$ on the lateral wall $(r = R)$ and by unity on the walls $z = 0$ and h.

5. THE ACOUSTIC PRESSURE AND PARTICLE VELOCITY FIELDS IN THE NON-ROTATING FLUID-FILLED CAVITY

5.1. THE PARTICLE VELOCITY: GENERAL EXPRESSION NEAR A WALL

The inertial factors (equation (25) and (26)) involve the expression of the whole "acoustic" particle velocity. This particle velocity is written as the sum of the laminar acoustic and laminar thermal velocities $\mathbf{v}_a$ and $\mathbf{v}_h$, and the vortical velocity $\mathbf{v}_v$. As mentioned in section 2 (equation (1)), the vortical component $\mathbf{v}_v$ of the particle velocity $\mathbf{v}$ plays an important role in the inertial coupling. This vortical velocity, like the thermal one, is negligible in comparison with the laminar acoustic velocity in the whole domain under consideration (the volume of the cavity) except in the boundary layers near the walls. On these walls, the particle velocity and the temperature variations vanish (equation (29)), namely $\mathbf{v}_a + \mathbf{v}_h + \mathbf{v}_v = \mathbf{0}$ and $\tau_a + \tau_h = 0$, and moreover, because the thermal and vortical velocities created on the boundaries by the acoustic perturbation are directly expressed in terms of diffusion process along the inward normal to the wall, these velocity components $\mathbf{v}_h$ and $\mathbf{v}_v$ die out over a very short distance from the wall (i.e., the boundary layer thicknesses denoted, respectively, as δ_h and δ_v), which are much lower than the height h and the radius R of the cavity. Hence, the periodic acoustic field outside the boundary layers is the solution of the set of equations (neglecting the bulk viscous and thermal effects as recommended above, section 4.2)

$$(\Delta + k_1^2)p_a = 0, \tag{47a}$$

with

$$\partial_u p_a = 0 \quad \text{on the walls}, \tag{47b}$$

the temperature variations and the acoustic velocity being given, respectively, by

$$\frac{\gamma - 1}{\hat{\beta}\gamma}\, p_a \quad \text{and} \quad \frac{\mathrm{i}}{\rho_0 \omega_1}\nabla p_a. \tag{47c, d}$$

These quantities, the acoustic pressure p_a, the temperature variation τ_a and the particle velocity $(\mathrm{i}/\rho_0\omega)\nabla p_a$, are considered below as the given external boundary expressions for the calculation of the velocity $\mathbf{v}$ and of the temperature fluctuations τ near a wall (inside the boundary layers) [10].

The linear equation which gives an accurate description of the small amplitude disturbances inside the viscous and thermal boundary layers must satisfy several assumptions in order to avoid overly intricate formulations, namely: (1) as the pressure variation can be assumed constant over the boundary layer thicknesses (because the wavelength is much greater than these thicknesses), the component normal (inwardly directed) to the wall considered v_u of the particle velocity $\mathbf{v}$ is much lower than its component $\mathbf{v}_w$ parallel to the wall, that is the flow is assumed to be essentially tangential to the wall and then, in the Navier–Stokes equation (21), the only $\mathbf{w}$-components tangential to the wall are considered (nevertheless, in order to assume the conservation of volume flow, the normal component of the velocity v_u has to be taken into account in the conservation of mass equation); (2) spatial variations in the normal direction $\mathbf{u}$ of both the velocity $\mathbf{v}$ and the temperature variation τ are much greater than spatial variations in tangential directions and hence the spatial variation of these quantities in the tangential directions can be neglected in the Navier–Stokes equation and in the Fourier heat conduction equation. Therefore, the complete set of equations and boundary conditions governing the fluid

motion inside the boundary layers, involving these approximations, is straightforwardly obtained from equations (21)–(23) (without rotation), leading to, for an harmonic perturbation,

$$\left[1 + \frac{1}{k_v^2}\,\partial_{uu}^2\right]\mathbf{v}_w(u, \mathbf{w}) = -\frac{1}{\mathrm{i}\omega_1\rho_0}\,\boldsymbol{\nabla}_w\, p(\mathbf{w}), \tag{48}$$

$$\mathrm{i}\omega_1\rho + \rho_0\boldsymbol{\nabla}\cdot\mathbf{v} = 0, \tag{49}$$

$$\left[1 + \frac{1}{k_h^2}\,\partial_{uu}^2\right]\tau = \frac{\gamma - 1}{\hat{\beta}\gamma}\; p, \tag{50}$$

$$\rho = \frac{\gamma}{c_0^2}\,(p - \hat{\beta}\tau), \qquad \tau(u = 0) = 0, \tag{51, 52}$$

$$v_u(u = 0) = 0 \quad \text{and} \quad \mathbf{v}_w(u = 0) = \mathbf{0}. \tag{53}$$

$$\mathbf{v}_w(u > \delta_v) = \frac{\mathrm{i}}{\rho_0\omega_1}\,\boldsymbol{\nabla}_w p_a\,, \qquad \tau(u > \delta_v) = \tau_a \tag{54, 55}$$

with $k_v = (1 - \mathrm{i})\sqrt{k_1/(2l'_v)}$ and $k_h = (1 - i)\sqrt{k_1/(2l_h)}$, where $u = 0$ means "on the wall considered". The solutions of equations (48) and (50), invoking equations (47) and subject to the boundary conditions (52)–(55) are given by

$$\mathbf{v}_w = \frac{\mathrm{i}}{\rho_0\omega_1}\,\boldsymbol{\nabla}_w p_a(1 - \mathrm{e}^{-\mathrm{i}k_v u}), \tag{56}$$

$$\tau = \frac{\gamma - 1}{\hat{\beta}\gamma} p_a(1 - \mathrm{e}^{-\mathrm{i}k_h u}), \tag{57}$$

the acoustic pressure p_a being considered here as a zero order expansion (with respect to the very small admittance β) of the pressure variation p (time dependence $\mathrm{e}^{\mathrm{i}\omega_1 t}$ is implicitly included in the factor p_a).

Combining these results and equations (49) and (51), along with equation (47a) that is $[\boldsymbol{\nabla}_w\cdot\boldsymbol{\nabla}_w + k_1^2]\,p_a = -\,\partial_{uu}^2 p_a$, yields

$$\rho = \frac{1}{c_0^2}\,[1 + (\gamma - 1)\,\mathrm{e}^{-\mathrm{i}k_h u}]\,p_a, \tag{58}$$

$$\partial_u v_u = \frac{\mathrm{i}}{\rho_0\omega_1}\partial_{uu}^2\, p_a - \left[\frac{k_w^2}{k_1^2}\,\mathrm{e}^{-\mathrm{i}k_v u} + (\gamma - 1)\mathrm{e}^{-\mathrm{i}k_h u}\right]\left(\frac{\mathrm{i}k_1}{\rho_0 c_0}\right) p_a, \tag{59}$$

where $k_w^2 p_a = -\,\boldsymbol{\nabla}_w\cdot\boldsymbol{\nabla}_w p_a$ ($\mathbf{k}_w$ being the component of the wave number $\mathbf{k_1}$ parallel to the wall), and then, taking into account that $(\partial_u p_a)_{(u > \delta_v)} \simeq 0$ (47d, 47b), the integration of equation (59) from $u = 0$ to every value of u greater or lower than the viscous or thermal boundary layer thicknesses (respectively, $\delta_v = \sqrt{2}/||k_v|| = \sqrt{2l'_v/k_1}$ and $\delta_h = \sqrt{2}/||k_h|| = \sqrt{2l_h/k_1}$) leads to

$$v_u = \frac{\mathrm{i}}{\rho_0\omega_1}\partial_u p_a + \left[\frac{k_w^2}{k_1^2}\frac{1}{\mathrm{i}k_v}(1 - \mathrm{e}^{-\mathrm{i}k_v u}) + \frac{(\gamma - 1)}{\mathrm{i}k_h}(1 - \mathrm{e}^{-\mathrm{i}k_h u})\right]\left(\frac{-\,\mathrm{i}k_1}{\rho_0 c_0}\right) p_a. \tag{60}$$

The "components" u (60) and $\mathbf{w}$ (56) of the vortical ($\mathbf{v}_v$) and thermal ($\mathbf{v}_h$) velocities are given by the factors involving $\mathrm{e}^{-\mathrm{i}k_v u}$ and $\mathrm{e}^{-\mathrm{i}k_h u}$ respectively. The sum of the other factors

represents the acoustic velocity in the visco-thermal fluid; for example the u-component of the acoustic velocity (equation 60)) is given by

$$v_{a_u} = \frac{\mathrm{i}}{\rho_0 k_1 c_0}\partial_u p_a - \left(\frac{k_w^2}{k_1^2}\frac{1}{\mathrm{i}k_v} + \frac{(\gamma-1)}{\mathrm{i}k_h}\right)\left(\frac{\mathrm{i}k_1}{\rho_0 c_0}\right)p_a. \tag{61}$$

It is noteworthy that the expression for $u = 0$ of the ratio $-\rho_0 c_0 v_{au}/p_a$ is equal to the specific admittance β introduced in equation (31) to express the boundary condition for the Green function in the frequency domain. Then, employing equation (61) and taking into account the property $(\partial_u p_a)_{u=0} = 0$, it follows that

$$\beta = k_1\left(\frac{k_w^2}{k_1^2}\frac{1}{k_v} + \frac{\gamma-1}{k_h}\right), \tag{62}$$

which is equal to the slightly transformed version for β given by equation (32) used in section 4.2. Moreover, this result is an *a posteriori* demonstration of the comments given in section 4.2 under equation (34).

5.2. THE ACOUSTIC FIELD IN THE NON-ROTATING CAVITY

With respect to the properties of the harmonic acoustic pressure field of the fluid-filled cavity at rest, the complete definition of the pressure variation p_a (equation (47)) implies that its own properties (spatial distribution, resonant frequency) are those of the Green function $\tilde{G}$ chosen in section 4.2, equation (42). It follows that, for the source strength given by equation (28), the analytical expression for the pressure variation p_a is given by

$$p_a(\mathbf{r}, t) = \mathrm{i}\omega_1 \rho_0 \mathrm{e}^{\mathrm{i}\omega_1 t} Q_0 \tilde{G}(R, \phi_0 = 0; r, \phi), \tag{63}$$

where only the eigenfunction ψ_1^c is involved in the Green function $\tilde{G}$.

Then the use of equations (38)–(42), along with the condition $k_{10}^2 - k_1^2 - \chi_1^2 = 0$ which implies that the cavity is excited at its resonance angular frequency $\omega_1 \simeq \omega_{10}$, yields

$$p_a = P_a \frac{\mathrm{J}_1(k_{10} r)}{\mathrm{J}_1(\gamma_{10})}\cos\phi\, \mathrm{e}^{\mathrm{i}\omega_{10} t}, \tag{64}$$

with

$$P_a = \frac{\rho_0 c_0^2 Q_0/\gamma_1}{(1 - 1/\gamma_{10}^2)\pi R^2 h}, \tag{65}$$

where γ_1 is given by equation (45).

Invoking equation (56), and considering the limits wherein first, the height h of the cavity is much greater than the boundary layer thicknesses (but much lower than the wavelength) and second, the radius is expected to approach infinity, the r- and ϕ-components of the particle velocity are expressed by

$$v_r^\infty = \frac{\mathrm{i}}{\rho_0 \omega_{10}}\partial_r p_a (1 - F_v), \tag{66}$$

$$v_\phi^\infty = \frac{\mathrm{i}}{\rho_0 \omega_{10}}\frac{1}{r}\partial_\phi p_a (1 - F_v), \tag{67}$$

with

$$F_v = \mathrm{e}^{-\mathrm{i}k_v z} + \mathrm{e}^{-\mathrm{i}k_v (h-z)} \tag{68}$$

and then, writing that R is the finite radius of the real cavity, equations (60) and (56) imply, respectively, that

$$v_r \simeq \frac{\mathrm{i}}{\rho_0 c_0}(1 - F_v) \tag{69}$$

$$\times \left[\frac{1}{k_{10}} \partial_r p_a + \left(\frac{1}{\gamma_{10}^2} \frac{k_{10}}{\mathrm{i}k_v} (1 - \mathrm{e}^{-\mathrm{i}k_v (R-r)}) + (\gamma - 1) \frac{k_{10}}{\mathrm{i}k_h} (1 - \mathrm{e}^{-\mathrm{i}k_h (R-r)}) \right) p_a \right],$$

$$v_\phi \simeq \frac{\mathrm{i}}{\rho_0 c_0}(1 - F_v) \left[\frac{1}{k_{10} r} (1 - \mathrm{e}^{-\mathrm{i}k_v (R-r)}) \partial_\phi p_a \right]. \tag{70}$$

Because the height h of the cavity is greater than the viscous boundary layer thickness $(1/\|k_v\|)$, the function $(1 - F_v)$ vanishes on the walls $z = 0$ and h, which therefore are not directly involved in the inertial modes coupling.

These results are appropriate to the particle velocity which satisfies the requirements involving the inertial forces mentioned in section 2, especially inside the boundary layers which play an important role in the acoustic effects of the non-uniform rotating flow Ω (as the vortical effect is emphasized by the term $\nabla \times \mathbf{v}$).

6. INERTIAL- AND FLOW-INDUCED ACOUSTIC MODES COUPLING IN THE UNSTEADY ROTATING CAVITY

6.1. SOLUTIONS FOR THE ACOUSTIC PRESSURE MEASURED

Discarding terms which depend on viscosity and thermal conduction (as indicated in section 4.2) and operators of orders higher than $(1/c_0^2)\delta\Omega\partial_\phi$ when operating on the acoustic pressure p, the set of equations (21)–(23) straightforwardly reduces to the propagation equation

$$\left[\Delta - \frac{1}{c_0^2} \partial_{tt}^2 \right] p = -\rho_0 \partial_t q + \frac{1}{c_0^2} [\partial_t \delta\Omega + 2\delta\Omega\partial_t] \partial_\phi p - \rho_0 \, \nabla \cdot \mathbf{\Gamma}, \tag{71}$$

the right-hand side of the equation being known upon assuming the Born approximation, that is by substituting into it results (64) and (69, 70) for the pressure variation and the particle velocity respectively.

The acoustic pressure variation is expressed as a sum of five terms:

$$p = p_a + p_{fl} + p_{co} + p_{aa} + p_{ce}, \tag{72}$$

which are governed, respectively, by propagation equations as follows (p_a and $\mathbf{v}$ being given by equations (64), (69) and (70): for the unperturbed acoustic pressure in the cavity at rest p_a (solution 64)) created by the loudspeaker

$$\left(\Delta - \frac{1}{c_0^2} \partial_{tt}^2 \right) p_a = -\rho_0 \partial_t q, \tag{73}$$

for the correction p_{fl} due to the effects of the non-uniform rotating flow on the acoustic pressure p_a

$$\left(\Delta - \frac{1}{c_0^2}\,\partial_{tt}^2\right) p_{fl} = \frac{1}{c_0^2}\left[\partial_t(\delta\Omega) + 2\delta\Omega\partial_t\right]\partial_\phi p_a, \tag{74}$$

for the perturbation p_{co} due to the Coriolis effect

$$\left(\Delta - \frac{1}{c_0^2}\,\partial_{tt}^2\right) p_{co} = 2\rho_0\left[\Omega(\nabla\times\mathbf{v})_z + v_\phi\partial_r\Omega\right], \tag{75}$$

where the right-hand side is equal to $(-\rho_0\nabla\cdot\mathbf{\Gamma}_c)$ (equation (26));

for the perturbation p_{aa} due to the effect of the angular acceleration,

$$\left(\Delta - \frac{1}{c_0^2}\,\partial_{tt}^2\right) p_{aa} = \frac{\rho_0}{\mathrm{i}\omega_{10}}\left[\partial_t\Omega(\nabla\times\mathbf{v})_z + v_\phi\partial_{rt}^2\Omega\right], \tag{76}$$

where the right-hand side is equal to $(-\rho_0\nabla\cdot\mathbf{\Gamma}_a)$ (equation 26));

for the perturbation p_{ce} due to the effect of the centripetal acceleration,

$$\left(\Delta - \frac{1}{c_0^2}\,\partial_{tt}^2\right) p_{ce} = \frac{\rho_0}{\mathrm{i}\omega_{10}}\left[\frac{1}{r}\,\Omega^2 v_r + 2v_r\Omega\partial_r\Omega + \mathbf{\Omega}^2\partial_r v_r + \frac{1}{r}\,\Omega^2\partial_\phi v_\phi\right], \tag{77}$$

where the right-hand side is equal to $(-\rho_0\nabla\cdot\mathbf{\Gamma}_e)$ (equation (26)).

It is noteworthy that the contributions of p_a and p_{ce} to the acoustic pressure vanish at $\phi = \pi/2$ (where the measurement microphone is located) because p_a, v_r, $\partial_r v_r$ and $\partial_\phi v_\phi$ involve only the eigenmode ψ_1^c which is proportional to $\cos\phi$ (see equations (64), (69) and (70)): at that position $\phi = \pi/2$, only p_{fl}, p_{ca} and p_{aa} have non-zero contribution to the acoustic field as these functions involve the eigenmode ψ_1^s which is proportional to $\sin\phi$. So, the function $(p_{fl} + p_{ca} + p_{aa})$ gives the pressure variation under consideration in the acoustic gyro.

Taking into account the properties of the Green function chosen (equation (43)), as regards the properties of the acoustic field in the cavity, the real parts of the solutions of equations (74), (75) and (76), denoted here indifferently as p_F, are given by the convolutions with respect to the four variables (r, ϕ, z, t) of their right-hand side (denoted here indifferently as $[-F(\mathbf{r}, t)]$) and the Green function G in the time domain restricted to the mode ψ_1^s (which does not vanish at $\phi = \pi/2$), namely

$$p_F(r,\phi,t) = \frac{c_0^2}{\omega_{10}}\,\mathscr{R}\left[\int_0^t \mathrm{d}t_0\,\mathrm{e}^{-\gamma_1(t-t_0)}\sin(\omega_{10}(t-t_0))\psi_1^s(\mathbf{r})\times\iiint_{(D)} F(\mathbf{r}_0,t_0)\psi_1^s(\mathbf{r}_0)\,\mathrm{d}\mathbf{r}_0\right]. \tag{78}$$

This result emphasizes that terms proportional to ψ_1^c in the function F does not contribute to the result p_F as a consequence of the orthogonality of the eigenfunctions ψ_1^c and ψ_1^s. In this solution, the integral along the t-axis lies on the definite interval $[0, t]$, the endpoints "0" and "t" being set, respectively, by the Heaviside step function $\mathrm{U}(t)$ in expressions (9)–(11) for Ω (included in the function F) and $\mathrm{U}(t - t_0)$ in expression (35) or (43) for the Green function G in the time domain, both being explicit representations of the causality. The triple integral is defined over the closed region (D) in space which represents the whole volume of the cavity.

The signal provided by the measurement microphone is analyzed with a lock-in amplifier (or equivalent) providing one with the amplitude of both the components in phase with the

primary signal ($\cos\omega_{10}t$, equation (28)) and the component in quadrature ($\sin\omega_{10}t$). In fact, it appears that only the in-phase component has to be considered (that is to say its root mean square) because the other one is negligible. Nevertheless, it is suitable to give explicit in-phase and in-quadrature representation of the measured signal. Moreover, as the variations of both the unsteady rotation velocity $\Omega(\mathbf{r}_0, t_0)$ included in the function F (the rotation rate Ω reaching the steady motion after several seconds) and the acoustic decay factor $e^{-\gamma_1(t-t_0)}$ (the wave created at each time damping out exponentially after several 10 ms) are much slower than the variation of the signal itself (the acoustic period being given by $2\pi/\omega_{10} \simeq 0{\cdot}1$ ms here), the functions which imply only cosine and sine of the variable $(\omega_{10}t_0)$ which appears in the integrand can be replaced by their mean value over their period $(2\pi\omega_1^{-1})$. This last assumption (sampling) greatly reduces the complexity of the analytic calculation (Appendix B). It allows to obtain numerically quickly with any personal computer, results involving more than 1000 terms in the Fourier–Bessel serie (equation (9)) for Ω, covering the transient period of the unsteady rotation, typically here 1 s. It also allows to obtain simple analytical results (after lengthy but tractable calculations) when the function Ω is expressed as a function of the complementary error function (equation (11)) valid for a time interval which covers the transient period of the gyro, here typically 100 ms), yielding, at the measurement point ($r = R$, $\phi = \pi/2$):

for the correction p_{fl} due to the effects of the non-uniform rotating flow on the acoustic pressure p_a

$$\frac{p_{fl}}{P_0}\left(R, \phi = \frac{\pi}{2}, t\right) \simeq -\left[(1 - e^{-\gamma_1 t})\frac{\gamma_{10}^2}{2}\left(1 - \frac{J_0(\gamma_{10})J_2(\gamma_{10})}{J_1^2(\gamma_{10})}\right) - \sqrt{\frac{2}{\pi}}\frac{\delta_v}{R}\sqrt{\omega_{10}t}\right]\cos\omega_{10}t, \tag{79}$$

$$\simeq -\left[1{\cdot}2(1 - e^{-\gamma_1 t}) - \sqrt{\frac{2}{\pi}}\frac{\delta_v}{R}\sqrt{\omega_{10}t}\right]\cos\omega_{10}t, \tag{80}$$

for the first term of the Coriolis perturbation (75), which depends on Ω,

$$\frac{p_{co}^{(\Omega)}}{P_0}\left(R, \phi = \frac{\pi}{2}, t\right) \simeq -(1 - e^{-\gamma_1 t})\cos\omega_{10}t, \tag{81}$$

for the second term of the Coriolis perturbation (75), which depends on $\partial_r\Omega$,

$$\frac{p_{co}^{(\partial_r\Omega)}}{P_0}\left(R, \phi = \frac{\pi}{2}, t\right) \simeq \left[(1 - e^{-\gamma_1 t}) - \frac{15}{8}\left(\frac{\delta_v}{R}\right)^2\omega_{10}t\right]\cos\omega_{10}t, \tag{82}$$

where

$$P_0 = \frac{4Q_f}{(\gamma_{10}^2 - 1)}\frac{\Omega_0}{\omega_{10}}P_a \tag{83}$$

is the acoustic pressure at the measurement microphone during the permanent regime, P_a being given by equation (65) and $Q_f = \omega_{10}/2\gamma_1$ being the quality factor.

The expression for p_{aa} is not given here as it is negligible compared with the contribution of perturbations (80)–(82) (it presents a very sharp shape near the origin of time, as expected because it depends on $\partial_t\Omega$ and $\partial_r\partial_t\Omega$).

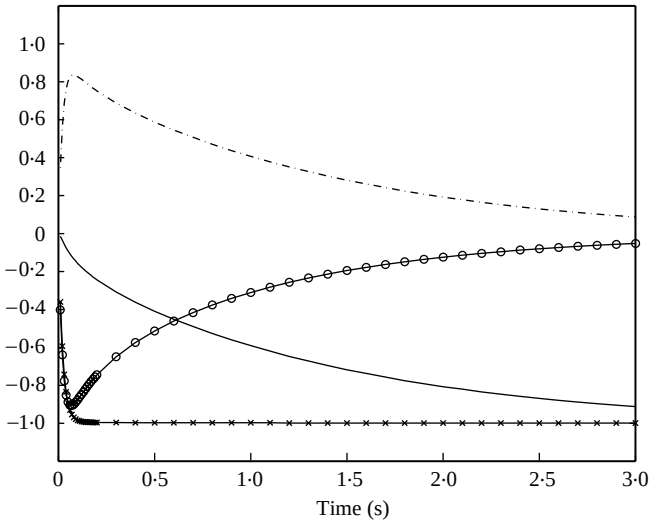

Figure 5. Root mean square amplitude of the normalized pressure (p_F/P_0) (equations (65) and (78)) as function of the time (transient responses), with the Fourier–Bessel expansion (9) for Ω. —○—, "fl": correction (p_{fl}/P_0) due to the effects of the non-uniform rotating flow on the acoustic pressure p_a; —×—, "co(Ω)": Coriolis acoustic perturbation ($p_{co}^{(\Omega)}/P_0$) which is proportional to Ω; ——, "co($\partial_r\Omega$)": Coriolis acoustic perturbation ($p_{co}^{(\partial_r\Omega)}/P_0$) which is proportional to $\partial_r\Omega$; ——, "co" : total Coriolis acoustic perturbation (sum of the two preceeding ones).

6.2. RESULTS, DISCUSSIONS AND CONCLUSION

For each contribution to the amplitudes of the pressure variations p_{fl}, $p_{co}^{(\Omega)}$ and $p_{co}^{(\partial_r\Omega)}$, discarding the second term on the right-hand side of solutions (80)–(82) which are negligible over the time interval from $t = 0$ until the contribution given by the decay factor $e^{-\gamma_1 t}$ dies out, the transient behaviour is given by the function $1 - e^{-\gamma_1 t}$: it is clearly governed by the acoustic transient of the cavity, that is the time period needed to stabilize the acoustic resonance, here roughly 100 ms. This result can be seen in Figure 5, curves "fl, co(Ω), co($\partial_r\Omega$)", Ω being given by its Fourier–Bessel expansion (9) in order to show the variations of each factor all over the unsteady rotation Ω of the fluid, the parameters used being given in Appendix C. These transient responses are not governed by the velocity distribution of the fluid rotation (with circular streamlines), generated by the rotation of the rigid boundaries, which reaches steady motion after more than 1 s here. Nevertheless, the contribution of the Coriolis effect $p_{co} = p_{co}^{\Omega} + p_{co}^{(\partial_r\Omega)}$ to the transient response of the gyro, given in Figure 5 (curve "co"), shows the sensitivity increasing regularly but slowly : this is confirmed by the first terms on the right-hand side of equations (81) and (82) which are the opposite to each other (this result is valid during the time period which covers the transient of the gyro, roughly 100 ms here). After that period the factor $p_{co}^{(\partial_r\Omega)}$ vanishes, and, as expected, the asymptotic value of the contribution $p_{co}^{(\Omega)}$ to the sensitivity of the transient response is exactly equal to the one obtained from the method used to calculate the steady state behaviour, which is itself in very good agreement with experimental results [2].

It is remarkable that the contribution of the correction term p_{fl} (equation (80)) is 1·2 times the contribution of the Coriolis term $p_{co}^{(\Omega)}$ (equation (81)) during the time period which covers the transient of the gyro ($\simeq$ 100 ms); one can say roughly that this term is opposite to the term $p_{co}^{(\partial_r\Omega)}$ in such a way that, during this period (early beginning) the only Coriolis pressure $p_{co}^{(\Omega)}$ gives, in first approximation, the behaviour of the gyro and that after this period this last term predominates as the others vanish. The theoretical (curve "th") and experimental [11] (curve "ex") results for the total pressure are shown in Figure 6; the

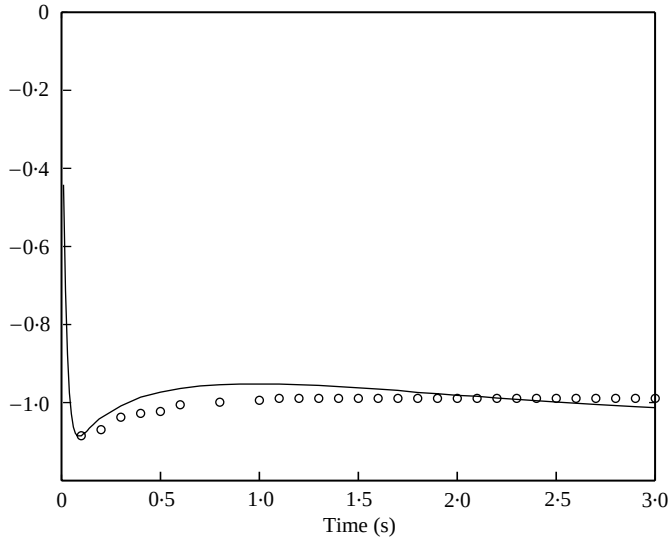

Figure 6. Root mean square of the amplitude of the normalized total acoustic pressure at the location of the measurement microphone ($r = R$, $\phi = \pi/2$) as a function of the time (transient response of the gyro). ——: theoretical results; ○: experimental results.

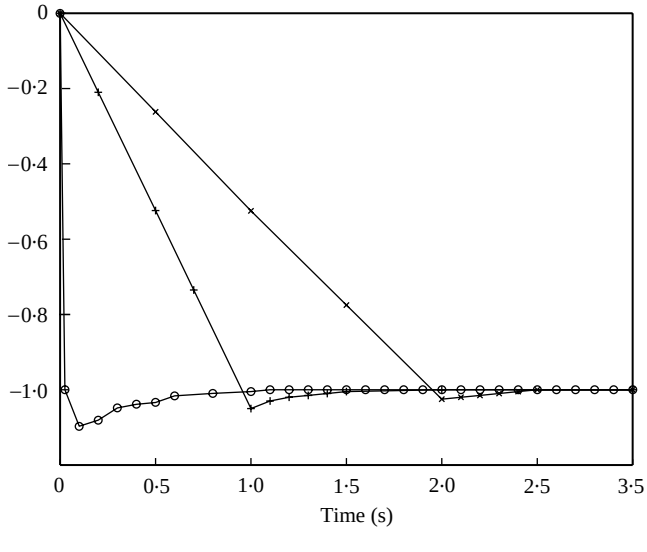

Figure 7. Root mean square of the amplitude of the normalized total acoustic pressure at the location of the measurement microphone ($r = R$, $\phi = \pi/2$) as a function of the time (transient response of the gyro). Experimental results for three rising times; —○—: $t_r = 0{\cdot}025$ s; —+—: $t_r = 1$ s; —×—: $t_r = 2$ s.

agreement is very good. The slight overstep around 100 ms can be explained by the factor $(\gamma_{10}^2/2)\ [1 - J_0(\gamma_{10})J_2(\gamma_{10})/J_1(\gamma_{10})^2] \simeq 1{\cdot}2$ on the right-hand side of equation (80), as mentioned in the above discussion. Note that the experimental results have been obtained by using a rotating table which can reach a rotation rate $\Omega_0 = 200^\circ/\text{s}$ after only 2·5 ms.

In conclusion, this paper provides a complete and quite simple model, not available until now, to describe the response of the acoustic gyro for strong variations of the rotation rates.

This model has been validated experimentally after several experiments which always confirm the experimental results given above: all of them show the special shape of the beginning of the transient (exceeding of the permanent regime level). Some experimental results are given in Figure 7, corresponding to different rising times: $t_r = 0{\cdot}025$, 1 and 2 s; the one that has been compared to the theoretical result is the shortest one.

The theoretical results convey an interpretation of the physical phenomena, namely the shape of the transient response and the characteristics of its stabilization time, giving the role played by each component of the inertial- and flow-induced acoustic modes coupling. Then finally, requirements that have to be taken into account in the design of acoustic gyros can now be addressed, using the theoretical results obtained in this work.

ACKNOWLEDGMENTS

This work has been funded by the Délégation Générale de l'Armement which has supported the research studentship of the first author when preparing his thesis that in part led to this paper.

REFERENCES

1. T. Bourouina, A. Exertier and S. Spirkovitch 1997 *Journal of Microelectromechanical Systems* **4**, 347–354. Preliminary results on a silicon gyrometer based on acoustic mode coupling in small cavities.
2. M. Bruneau, C. Garing and H. Leblond 1986 *Journal of the Acoustical Society of America* **80**, 672–680. A rate gyro based on acoustic mode coupling.
3. Ph. Herzog and M. Bruneau 1989 *Journal of the Acoustical Society of America* **86**, 2377–2384. Shape perturbation and inertial mode coupling in cavities.
4. P. Hameby, Ph. Dupire and M. Bruneau 1997 *Acta Acustica* **83**, 13–18. Acoustic fields in trapezoidal cavities.
5. M. Bruneau, A. M. Bruneau and Ph. Dupire 1995 *Acta Acustica* **3**, 275–282. A model for rectangular miniaturized microphones.
6. Ph. Dupire and M. Bruneau 1998 *Journal of Sound Vibration* **212**, 37–59. Transient behaviour of the acoustic rate gyro.
7. G. K. Batchelor 1967 *An Introduction to Fluid Dynamics*. Cambridge: Cambridge University Press.
8. H. S. Carslaw and J. C. Jaeger 1959 *Conduction of Heat in Solids*. Oxford: Oxford University Press; second edition.
9. M. Bruneau 1998 *Manuel d'acoustique fondamentale*. Paris: Hermès.
10. N. Rott 1974 *Journal of Applied Mathematics and Physics* **25**, 417–421. The influence of heat condition on acoustic streaming.
11. Private communication from Sextant-Avionique company. *Technical Report*.
12. M. Abramovitz and I. Stegun 1964 *Handbook of Mathematical Functions*. New York: Dover Publications.
13. R. C. Reid 1986 *The Properties of Gases and Liquids*. New York: McGraw-Hill.

APPENDIX A: SIMPLIFIED ANALYTICAL EXPRESSION OF THE ROTATION RATE, FOR SMALL TIME INTERVAL FROM THE ORIGIN $t = 0$

A.1. ROTATION RATE CLOSE TO THE PLANE WALLS $z = 0$ OR h

Near the plane walls $z = 0$ and h, for small time interval near the origin (i.e., for time interval which covers the transient period of the gyro, here about 100 ms), the azimuthal

component of the fluid velocity V_θ can be assumed to be both independent of the r and θ co-ordinates (except in the corner of the cavity). Thus, equation (7) and the associated boundary conditions (8a) that govern the velocity distribution are, respectively, written as

$$\left(\frac{\partial}{\partial t} - \nu\frac{\partial^2}{\partial z^2}\right)V_\theta = 0 \quad \text{near the surfaces } z = 0 \text{ and } z = h, \tag{A.1}$$

$$V_\theta(z = 0 \text{ or } z = h, t) = \Omega_0 R U(t) \quad \text{on the surface } z = 0 \text{ or } z = h. \tag{A.2}$$

These equations are equivalent to those of the problem of a plane boundary suddenly set in translation parallel to its plane in a fluid at rest [7], whose solution near the plane walls leads to

$$\frac{\Omega^{(0/h)}}{\Omega_0} = \operatorname{erfc}\left(\frac{x}{2\sqrt{\nu t}}\right)\mathrm{U}(t), \tag{A.3}$$

where $x = 0$ or $h - z$, respectively, near the surfaces $z = 0$ and h, and where $\operatorname{erfc}(y) = 1 - (2/\pi)\int_0^y \mathrm{e}^{-u^2}\,\mathrm{d}u$ is the complementary error function.

A.2. ROTATION RATE CLOSE TO THE LATERAL CYLINDRICAL WALL ($r = R$), FOR SMALL TIME INTERVAL FROM $t = 0$

Close to the lateral cylindrical wall ($r = R$), the azimuthal component of the fluid velocity V_θ is assumed to be independent of the z co-ordinate. The velocity distribution is still governed by the diffusion equation (7) that takes the form

$$\left(\frac{\partial^2}{\partial r^2} + \frac{1}{r}\frac{\partial}{\partial r} - \frac{1}{r^2} - \frac{1}{\nu}\frac{\partial V_\theta}{\partial t}\right)V_\theta = 0. \tag{A.4}$$

The Laplace transform of equation (A.4), along with the associated boundary conditions (8b), gives the following subsidiary system (taking into account that $V_\theta(t = 0, r < R) = 0$):

$$\left(\frac{\partial^2}{\partial r^2} + \frac{1}{r}\frac{\partial}{\partial r} - \frac{1}{r^2} - \kappa^2\right)\bar{V}_\theta = 0 \quad \text{for } 0 \leqslant r < R, \tag{A.5}$$

$$\bar{V}_\theta = \frac{\Omega_0 R}{s} \quad \text{for } r = R, \quad \text{and } \bar{V}_\theta \text{ finite at } r = 0, \tag{A.6}$$

where s is the Laplace variable, $\bar{V}_\theta$ the Laplace transform of V_θ, with $\kappa^2 = s/\nu$. The solution of this set of equations is given by

$$\bar{V}_\theta = \frac{\Omega_0 R}{s}\frac{\mathrm{I}_1(\kappa r)}{\mathrm{I}_1(\kappa R)}, \tag{A.7}$$

where I_1 is the first order modified Bessel function of the first kind. Then, using properties of the Laplace transformation and the asymptotic expansion of the Bessel function $\mathrm{I}_1(u) = (\mathrm{e}^u/\sqrt{2\pi u}(1 - 3/(8u) + \cdots) + o(\mathrm{e}^u)$, the expression of V_θ for small values of $(\nu t/R^2)$ takes the approximate form

$$V_\theta(t) = \Omega_0 R\sqrt{R/r}\left[\operatorname{erfc}\left(\frac{R - r}{2\sqrt{\nu t}}\right) - \frac{3}{8}\sqrt{\nu t}\,\frac{(R - r)}{Rr}\,2\int_{(R-r)/2\sqrt{\nu t}}^{\infty}\operatorname{erfc}(u)\,\mathrm{d}u\right]$$

$$\approx \Omega_0 R\sqrt{\frac{R}{r}}\operatorname{erfc}\left(\frac{R - r}{2\sqrt{\nu t}}\right) \tag{A.8}$$

giving an approximate expression of the rotation rate $\Omega^{(R)}$ near the cylindrical lateral wall valid in a small time interval from $t = 0$ ($0 < t < 300$ ms in our application):

$$\frac{\Omega^{(R)}}{\Omega_0} = \left(\frac{R}{r}\right)^{3/2} \operatorname{erfc}\left(\frac{R-r}{2\sqrt{\nu t}}\right) \mathrm{U}(t). \tag{A.9}$$

APPENDIX B: ANALYTICAL EXPRESSION OF THE ACOUSTIC PRESSURE VARIATION (72): THE CORIOLIS PERTURBATION ($p_{co}^{(\Omega)}$) (PROPORTIONAL TO Ω, EQUATION (75))

This appendix is given as an example of the calculations which lead to the analytical expressions that are obtained for the acoustic pressure variation (72). It deals only with the first term of the Coriolis perturbation ($p_{co}^{(\Omega)}$) which depends on Ω (equation (75)), because it can be easily extended to the other terms p_{fl} and $p_{co}^{(\partial_r \Omega)}$.

B.1. GENERAL EXPRESSION

The expression of the acoustic pressure due to the Coriolis perturbation proportional to Ω is given by the general equation (78) considering $F = -2\rho_0 \Omega(\nabla \wedge \mathbf{v})_z$ (equation (75)):

$$p_{co}^{(\Omega)}(r, \phi, t) = -\frac{c_0^2}{\omega_{10}} \mathscr{R}\left[\int_0^t \mathrm{d}t_0 \, \mathrm{e}^{-\gamma_1(t-t_0)} \sin(\omega_{10}(t-t_0)) \psi_1^s(\mathbf{r}) \times \iiint_{(D)} 2\rho_0 \Omega(\nabla \wedge \mathbf{v})_z \psi_1^s(\mathbf{r}_0) \, \mathrm{d}\mathbf{r}_0 \right]. \tag{B.1}$$

Assuming that the viscous and thermal boundary layers are much smaller than the acoustic wavelength (i.e., $k_v \gg k_{10}$ and $k_h \gg k_{10}$), and taking into account that the coupling factor $(\nabla \wedge \mathbf{v})_z$ involves only the vortical component $\mathbf{v}_v$ of the acoustic velocity $\mathbf{v}$ (equations 69–70), it takes the the form $(\nabla \wedge \mathbf{v})_z = (\nabla \wedge \mathbf{v}_v)_z \approx (k_v/\rho_0 \omega_{10}))\, \mathrm{e}^{-\mathrm{i}k_v(R-r)} (1/r)\, \partial_\phi p_a$.

Then, giving both the expressions of the eigenfunctions ψ_1^s (equations (39–41)) and the acoustic pressure p_a, equation (64), the integration of expression (B.1) with respect to the ϕ co-ordinate, for any expression of the rotation rate Ω equation (11 or 9), yields at the measurement point ($r = R$, $\phi = \pi/2$)

$$\frac{p_{co}^{(\Omega)}}{P_0}\left(R, \frac{\pi}{2}, t\right) = \mathscr{R}\left[\int_0^t \mathrm{e}^{-\gamma_1(t-t_0)} \sin(\omega_{10}(t-t_0)) \mathrm{e}^{\mathrm{i}\omega_{10}t_0} \times \int_0^R 2\left(\frac{\mathrm{J}_1((\gamma_{10}/R)r_0)}{\mathrm{J}_1(\gamma_{10})}\right)^2 k_v \mathrm{e}^{-\mathrm{i}k_v(R-r_0)} \right.$$
$$\left. \times \left(\frac{1}{h}\int_0^h (1 - F_v)\frac{\Omega}{\Omega_0} \mathrm{d}z_0\right) \mathrm{d}r_0 \, \mathrm{d}t_0 \right], \tag{B.2}$$

where P_0 is the acoustic pressure at the measurement microphone, for the steady state regime, given by equation (83).

The term F_v (equation (68)) is negligible everywhere outside the thin viscous boundary layers near the surface $z = h$ and 0. Then, inside the whole integration domain $[0, h]$ with respect to the z co-ordinate, its contribution can be neglected, which leads to the approximation $\int_0^h (1 - F_v)(\Omega/\Omega_0)\, \mathrm{d}z_0 \simeq \int_0^h (\Omega/\Omega_0)\, \mathrm{d}z_0$.

Moreover, assuming that the acoustic and inertial transient phenomena vary much slower than the acoustic signal, the functions which depend on the variable $\omega_{10} t_0$ can be

replaced by their mean value over one acoustic period $2\pi/\omega_{10}$: then equation (B.3) becomes

$$\frac{p_{co}^{(\Omega)}}{P_0}\left(R, \frac{\pi}{2}, t\right) = \mathscr{R}\left[\frac{1}{2}(\sin(\omega_{10}t)) - \mathrm{i}\cos(\omega_{10}t))\int_0^t \mathrm{e}^{-\gamma_1(t-t_0)} \times \int_0^R 2\left(\frac{\mathrm{J}_1((\gamma_{10}/R)r_0)}{\mathrm{J}_1(\gamma_{10})}\right)^2 k_v \mathrm{e}^{-\mathrm{i}k_v(R-r_0)}\left(\frac{1}{h}\int_0^h \frac{\Omega}{\Omega_0}\mathrm{d}z_0\right)\mathrm{d}r_0\,\mathrm{d}t_0\right] \tag{B.3}$$

and can be expressed in terms of two components as

$$\frac{p_{co}^{(\Omega)}}{P_0}\left(R, \frac{\pi}{2}, t\right) = A_c\cos(\omega_{10}t) + A_s\sin(\omega_{10}t), \tag{B.4}$$

where the in-phase component and the component in quadrature take, respectively, the approximate forms

$$A_c = -\gamma_1\int_0^t \mathrm{e}^{-\gamma_1(t-t_0)}\int_0^{R/\delta_v}\left(\frac{\mathrm{J}_1[\gamma_{10}(1-(\delta_v/R)u)]}{\mathrm{J}_1(\gamma_{10})}\right)^2\sqrt{2}\,\mathrm{e}^{-u}\cos\left(\frac{\pi}{4}-u\right) \times\left(\frac{1}{h}\int_0^h\frac{\Omega}{\Omega_0}\mathrm{d}z_0\right)\mathrm{d}u\,\mathrm{d}t_0, \tag{B.5}$$

$$A_s = -\gamma_1\int_0^t \mathrm{e}^{-\gamma_1(t-t_0)}\int_0^{R/\delta_v}\left(\frac{\mathrm{J}_1[\gamma_{10}(1-(\delta_v/R)u)]}{\mathrm{J}_1(\gamma_{10})}\right)^2\sqrt{2}\,\mathrm{e}^{-u}\sin\left(\frac{\pi}{4}-u\right) \times\left(\frac{1}{h}\int_0^h\frac{\Omega}{\Omega_0}\mathrm{d}z_0\right)\mathrm{d}u\,\mathrm{d}t_0, \tag{B.6}$$

upon setting $u = (R - r)/\delta_v$.

Numerical results with no time limitations (see section 6.2) can be obtained from these last expressions.

B.2. APPROXIMATE EXPRESSION

Furthermore, for small time intervals from $t = 0$, expression (11) leads to the following simplified expressions:

$$A_c \simeq -\gamma_1\int_0^t \mathrm{e}^{-\gamma_1(t-t_0)}\int_0^{R/\delta_v}\left(\frac{\mathrm{J}_1[\gamma_{10}(1-(\delta_v/R)u)]}{\mathrm{J}_1(\gamma_{10})}\right)^2\sqrt{2}\,\mathrm{e}^{-u}\cos\left(\frac{\pi}{4}-u\right) \times\mathrm{erfc}\left(\frac{R-r_0}{2\sqrt{\nu t_0}}\right)\mathrm{d}u\,\mathrm{d}t_0, \tag{B.7}$$

$$A_s \simeq -\gamma_1\int_0^t \mathrm{e}^{-\gamma_1(t-t_0)}\int_0^{R/\delta_v}\left(\frac{\mathrm{J}_1[\gamma_{10}(1-(\delta_v/R)u)]}{\mathrm{J}_1(\gamma_{10})}\right)^2\sqrt{2}\,\mathrm{e}^{-u}\sin\left(\frac{\pi}{4}-u\right) \times\mathrm{erfc}\left(\frac{R-r_0}{2\sqrt{\nu t_0}}\right)\mathrm{d}u\,\mathrm{d}t_0, \tag{B.8}$$

where the term e^{-u} implies that the integrand of the integral with respect to the u-co-ordinate normal to the boundary is negligible everywhere outside the viscous boundary

layer (i.e., $u \gg 1$). Then, inside this boundary layer, the Bessel function J_1 can be replaced by its Taylor expansion around $u \simeq 0$, $J_1(\gamma_{10}[1-(\delta_v/R)u]) \simeq J_1(\gamma_{10})$, which allows one to simplify the calculation of the integral along the u-co-ordinate, leading to

$$A_c = -\gamma_1 \int_0^t e^{-\gamma_1(t-t_0)} \times [1-(1-C-S)\cos(\omega_{10}t_0) - (C-S)\sin(\omega_{10}t_0)\,dt_0], \quad \text{(B.9)}$$

$$A_s = -\gamma_1 \int_0^t e^{-\gamma_1(t-t_0)} \times [-(1-C-S)\sin(\omega_{10}t_0) + (C-S)\cos(\omega_{10}t_0)\,dt_0], \quad \text{(B.10)}$$

where $C = C(\sqrt{2\omega_{10}t_0/\pi})$ and $S = S(\sqrt{2\omega_{10}t_0/\pi})$ are the Fresnel integrals defined by $C(y) = \int_0^y \cos^2(\pi t^2)\,dt$ and $S(y) = \int_0^y \sin^2(\pi t^2)\,dt$.

Moreover, the use of the appropriate Fresnel integrals approximate properties [12] greatly simplifies the expressions for the two components A_c and A_s:

$$A_c \simeq -\gamma_1 \int_0^t e^{-\gamma_1(t-t_0)} \left(1 + \frac{1}{2}\sqrt{\frac{2}{\pi\omega_{10}t_0}}\right) dt_0 = -[1-e^{-\gamma_1 t}], \quad \text{(B.11)}$$

$$A_s \simeq \gamma_1 \int_0^t e^{-\gamma_1(t-t_0)} \frac{1}{2}\sqrt{\frac{2}{\pi\omega_{10}t_0}}\Big) dt_0$$

$$= \gamma_1 \frac{e^{-\gamma_1 t}}{\sqrt{2\omega_{10}}} (-\gamma_1)^{-1/2} \operatorname{erfc}(i\sqrt{\gamma_1 t}). \quad \text{(B.12)}$$

Finally, as the component in quadrature appears to be always much smaller than the in-phase component, the expression for the first term of the Coriolis perturbation ($p_{co}^{(\Omega)}$), for small time interval from the origin $t = 0$, takes the following approximate form:

$$\frac{p_{co}^{(\Omega)}}{P_0}(R, \tfrac{1}{2}\pi, t < 300\text{ ms}) \simeq -(1-e^{-\gamma_1 t})\cos(\omega_{10}t). \quad \text{(B.13)}$$

with

$$P_0 = \frac{4Q_f}{\gamma_{10}^2 - 1}\frac{\Omega_0}{\omega_{10}} P_a. \quad \text{(B.14)}$$

APPENDIX C: VALUES OF THE GEOMETRICAL AND PHYSICAL PARAMETERS USED

This appendix contains the data used in the numerical simulations and the experimental set-up (see section 6.2).

Geometrical parameters of the cavity:
$R = 0{\cdot}007$ m radius of the cylindrical cavity: $h = 0{\cdot}004$ m height of the cylindrical cavity.

Physical parameters of the fluid SF6 [13]:
$M = 146 \times 10^{-3}\ \text{kg mol}^{-1}$ molar mass;
$\rho_0 = 14{\cdot}6\ \text{kg m}^{-3}$ density (2·5 bar, 300 K);
$C_p = 91{\cdot}5\ \text{J mol}^{-1}\,K^{-1}$ heat coefficient at constant pressure per unit of mass of the fluid (300 K);
$\gamma = 1{\cdot}1$ specific heat ratio (300 K);

$v = 9{\cdot}3 \times 10^{-7}$ m^2/s coefficient of kinematic viscosity of the fluid (300 K);
$\lambda = 13{\cdot}4 \times 10^{-3}$ W/m/K coefficient of thermal conductivity of the fluid, (2·5 bar, 300 K);
$c_0 = 135$ m/s adiabatic speed of sound (2·5 bar, 300 K).

Experimental parameters:
$P_0 = 2{\cdot}5 \times 10^5$ Pa static pressure;
$T_0 = 300$ K static temperature;
$\Omega_0 = 3{\cdot}5$ rad/s angular frequency of the walls of the cavity.

Other parameters:
$\delta_v = 7{\cdot}3 \times 10^{-6}$ m viscous boundary layer thickness;
$\omega_{10} = (1{\cdot}84/R)\, c_0 = 35\,485$ rad/s working angular frequency;
$\gamma_1^{-1} = 2 \times 10^{-2}$ s reverberation time;
$\hat{\beta} = P_0/T_0 = \text{kg m}^2\,\text{K}^{-1}$ increase in pressure per unit increase in temperature at constant density;
$\chi_T = 1/P_0 = 4 \times 10^{-6}\ \text{Pa}^{-1}$ isothermal compressibility.